BULLETIN OF THE POLISH ACADEMY OF SCIENCES
TECHNICAL SCIENCES, Vol. 74(3), 2026, Article number: e157566
DOI: 10.24425/bpasts.2026.157566

The influence of preparation methods and doping on piezoelectric properties induced by the electric field for potassium bismuth titanate $K_{0.5}Bi_{0.5}TiO_3$

Piotr RAKUS[1]*, **Jaroslaw JEDRYKA**[1], **Piotr CZAJA**[2], **and Katarzyna OSINSKA**[3]

[1] Faculty of Electrical Engineering, Czestochowa University of Technology, Armii Krajowej 17, PL-42-201, Częstochowa, Poland
[2] Institute of Technology, University of the National Education Commission, Krakow, Poland
[3] Faculty of Science and Technology, Institute of Materials Engineering, University of Silesia in Katowice, Poland

Abstract. In this article, the influence of processing conditions, dopant type and poling temperature on the microstructure and piezoelectric behavior of lead-free $K_{0.5}Bi_{0.5}TiO_3$ (KBT) ceramics is presented. Base KBT samples and those doped with Sr, Ca and Mn were synthesized via a solid-state reaction route, and examined with respect to their structural characteristics and electromechanical response. Particular emphasis was placed on elevated-temperature poling and its interaction with grain morphology and defect chemistry. SEM observations were used to identify dopant-dependent microstructural variations, while measurements of the d_{33} coefficient provided insight into how these factors influence efficiency of the poling process. The study demonstrates the importance of jointly optimizing synthesis parameters, dopant selection and poling conditions when tailoring the functional properties of KBT-based piezoelectric ceramics.

Keywords: potassium bismuth titanate (KBT); piezoelectric coefficient; ceramic microstructure; electric field polarization; lead-free piezoelectrics.

1. INTRODUCTION

In the era of rapid development in smart materials technology, piezoelectric ceramics are increasingly used in microelectromechanical systems (MEMS), sensors, actuators and energy-conversion devices [1–5]. Their functional performance depends strongly on microstructure, domain configuration and the presence of defects or dopants, all of which influence electromechanical coupling [3, 6–9]. In polycrystalline materials, grain size, porosity and local structural distortions play a key role in determining dielectric and piezoelectric behavior [3, 10–13]. Although lead-based systems such as PZT and PMN-PT exhibit exceptionally high piezoelectric coefficients [2, 6, 11, 14], increasing ecological and regulatory pressure has intensified research into lead-free alternatives. Compounds such as BNT, BZT and BZT-BCT demonstrate promising properties [15–19], yet they often require complex processing routes or compositional optimization to reach performance levels comparable to lead-based materials. Among environmentally friendly perovskites, potassium bismuth titanate $K_{0.5}Bi_{0.5}TiO_3$ (KBT) stands out due to its stable ferroelectricity, high Curie temperature and potential for further modification through controlled doping and processing [20–22]. Electric-field poling remains an essential step in activating the piezoelectric response in ceramic materials such as PZT [14, 23–26]. However, in lead-free systems including KBT the efficiency of poling depends strongly on microstructure and defect chemistry. Temperature, sintering conditions and dopant type influence grain growth, porosity and domain mobility, thereby affecting the achievable d_{33} values. The combined impact of preparation route, dopant selection (Sr, Ca, Mn) and poling temperature on the resulting d_{33} coefficient in KBT ceramics remains insufficiently understood. Existing studies typically investigate these factors separately, leaving a gap in understanding their synergistic effects. The aim of this work is to systematically evaluate how grinding time, sintering conditions and selected dopants influence the microstructure and piezoelectric properties of KBT ceramics, with particular emphasis on the enhancement of the d_{33} coefficient under elevated-temperature poling. To the best of our knowledge, no systematic study has simultaneously evaluated the influence of preparation route, dopant chemistry and elevated-temperature poling on the piezoelectric response of KBT ceramics.

2. PREPARATION OF $K_{0.5}Bi_{0.5}TiO_3$ MATERIAL

$K_{0.5}Bi_{0.5}TiO_3$ (KBT) is a lead-free perovskite-type material (ABX_3) in which the A-site is occupied by larger cations such as K^+ or Bi^{3+}, while the B-site contains smaller transition-metal ions such as Ti^{4+} or $Mn^{3+/4+}$. The oxygen octahedra (BX_6) form a typical perovskite framework widely used in functional materials, including energy-related applications [27]. KBT exhibits two structural phase transitions at approximately 683 K (cubic → pseudocubic) and 573 K (pseudocubic → tetragonal), and its Curie temperature (~ 643 K) is lower than that of

*e-mail: piotr.rakus@pcz.pl

Manuscript submitted 2025-04-11, revised 2025-12-11, initially accepted for publication 2026-01-01, published in May 2026.

$PbTiO_3$ or $Bi_4Ti_3O_{12}$ [20, 28]. Grinding time is known to influence microstructural homogeneity, leading to more uniform grain size distribution [21, 22]. In this work, undoped KBT and KBT doped with 0.5 mol% of Sr, Ca and Mn were synthesized using a conventional solid-state reaction route. High-purity precursors ($TiO_2 \geq 99.0\%$, $Bi_2O_3 \geq 99.9\%$, K_2CO_3, $SrCO_3 \geq 99.9\%$, $CaCO_3 \geq 99.9\%$, $MnO_2 \geq 99.9\%$) were mixed in stoichiometric proportions. Potassium carbonate, due to its hygroscopic nature, was pre-heated to remove moisture. For the base KBT, powders were milled for 2, 4 and 12 hours, calcined at 1173 K, re-milled, pressed at 100 MPa and sintered at 1318 K. The resulting samples were labelled KBT (2h + 2h), KBT (4h + 4h) and KBT (12h + 12h). For the doped materials (KBT:Sr, KBT:Ca, KBT:Mn), the synthesis involved three sintering stages at 1073 K, 1253 K, and 1303 K, combined with intermediate milling steps. All samples were pressed at 100 MPa. The final ceramics achieved relative densities of 96–98%, confirmed by the Archimedes method [29–31].

3. MEASURING STATION AND RESULTS

The samples were polarized using a standard high-field procedure with an applied electric field of 1.5 kV/mm and a poling time of 10 minutes. The process was carried out at 523 K, selected to remain below the Curie temperature while allowing increased dipole mobility. The description of the measurement configuration has been limited to information necessary to reproduce the experiment.

The measurements were performed using a YE2730A piezoelectric meter, which is used to directly measure the piezoelectric constant d_{33} for piezoelectric ceramics, polymers and single crystals. Longitudinal coefficient d_{33} represents the induced electric displacement along the poling axis (axis 3) per unit of applied stress in the same direction. In contrast, d_{31} and d_{32} describe the response along axis 3 when the stress is applied along axes 1 or 2, respectively. The device measures d_{33} values over a very large measuring range, with a high level of resolution and reliability. Measurement accuracy varies by ±2% of the d_{33} value in the range from 1 to 200 pC/. Before polarizing the samples, their orientation was initially checked at ambient temperature (295 K). In all cases it was 0 pC/N, which meant anisotropy of the electric dipole arrangement. The samples were placed between high-voltage electrodes in a Teflon fixture (Fig. 1). After

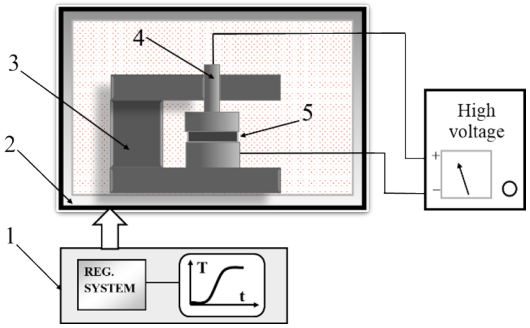

Fig. 1. Diagram of the station for polarization of piezoelectric materials in an electric field and elevated temperature: 1 – temperature controller with timer, 2 – chamber, 3 – electrode holder, 4 – electrode, 5 – sample

poling, the samples were cooled to room temperature under the applied field, after which the d_{33} value was measured. Then the d_{33} parameter was measured several times in different places of the sample. The average results are presented in Table 1. The next step was to introduce the polarizing system together with the sample into a chamber with regulated temperature and annealing time set at 10 minutes. After reaching the target temperature (below the Curie point), high voltage was switched on. After the set time had elapsed, the chamber power supply was disconnected and the system went into cooling mode with the HV switched on. After complete cooling to ambient temperature, the d_{33} value was read again several times. The average results are presented in Table 2. Measurement parameters: sample thickness: from 1 mm to 3 mm; diameter 10 and 15 mm; electric field intensity 1.5 kV/mm; polarization time: 10 min at 523 K. Polarization voltage was maintained until completely cooled.

In the case of measurements of the d_{33} parameter for samples polarized at ambient temperature, a reduction of the d_{33} value by several percent was observed in relation to the maximum value read in the first seconds of the measurement. Table 2 presents the average results of measurements of the d_{33} parameter for the samples polarized at the temperature of 523 K. In contrast to the samples polarized at ambient temperature, the fluctuations of the d_{33} parameter value were insignificant (0.5–1 pC/N), but a significant increase in its value was observed.

Table 3 presents the values of the d_{33} parameter increase for samples polarized at 523 K relative to 295 K. The largest in-

Table 1

Changes of the d_{33} parameter for the base and doped samples polarized at ambient temperature

Material	KBT 2h + 2h	KBT 4h + 4h	KBT 12h + 12h	KBT:Sr	KBT:Ca	KBT:Mn
d_{33} [pC/N]	19.1	21.0	17.1	40.1	27.0	28.2

Table 2

Changes of the d_{33} parameter for the base and doped samples polarized at elevated temperature

Material	KBT 2h + 2h	KBT 4h + 4h	KBT 12h + 12h	KBT:Sr	KBT:Ca	KBT:Mn
d_{33} [pC/N]	39.4	32.0	25.1	53.0	37.0	35.0

Table 3

Differences in the d_{33} parameter values for base and doped KBT materials polarized under various temperature conditions (523 K and 295 K)

Material	KBT 2h + 2h	KBT 4h + 4h	KBT 12h + 12h	KBT:Sr	KBT:Ca	KBT:Mn
Δd_{33} [%]	119.0	52.4	47.0	75.4	29.0	24.1

crease in relative value was observed for KBT 2h + 2h taking into account the base samples, and for KBT:Sr with respect to the doped samples. To explain the stronger enhancement of d_{33} in Sr-doped KBT as compared to Ca or Mn-doped KBT, we observe that the isovalent A-site Sr^{2+} ion optimizes the tolerance factor and reduces A-site random fields. This facilitates domain wall mobility during poling. The smaller Ca^{2+} ion increases octahedral tilts and elastic pinning, whereas the Mn^{2+} ion, acting as an acceptor, typically forms defect-dipole complexes ($Mn-V_O$) that stabilize domain walls and limit the extrinsic contribution to d_{33}. Together with microstructural differences (grain size and densification), these effects are consistent with the trend observed in [21, 22]. Poling at 523 K (below the tetragonal-to-pseudocubic transition temperature of ~ 573 K in KBT) reduces the coercive field and increases domain wall/dipole mobility. This enables more complete alignment and a higher remanent polarization after cooling. Accordingly, the measured d_{33} increases with poling temperature within the range of 295–523 K (Fig. 2), which is consistent with the reported structural and dielectric softening of KBT as it approaches the transition temperature [32].

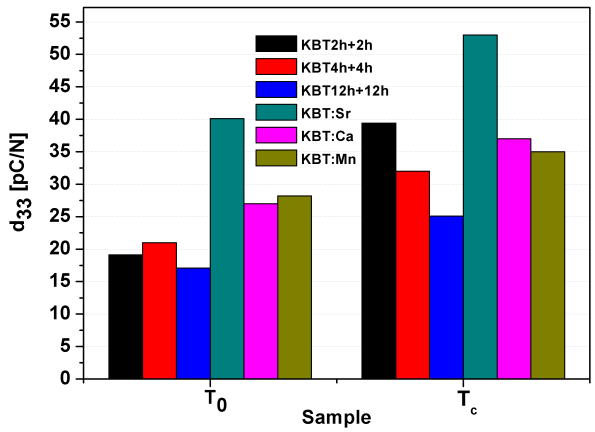

Fig. 2. Influence of polarization at elevated temperature on the d_{33} parameter value for base and doped samples

A significant effect of temperature on the value of the d_{33} parameter was observed – increase (24.1–119.0%). Due to significant differences in the d_{33} parameter values depending on the production process and doping, microscopic observations of sample fractures were also performed using a scanning electron microscope to reveal their morphology. SEM images presented in Fig. 3 illustrate the fracture structure of selected samples: base material (a) and doped materials (b, c, d). These images were captured under identical sintering conditions – 1318 K for the base material and 1303 K for the doped samples, with sintering time of 6 hours. The microstructure's shape and form play a crucial role in determining the material's physical and electrical properties, notably the piezoelectric coefficient d_{33}. The elevated-temperature poling (523 K) led to significant improvements in piezoelectric performance, particularly in the samples doped with Sr. This can be attributed to the enhanced mobility of domain walls at higher temperatures, which allows for more efficient polarization. The temperature-dependent behavior observed in this study is consistent with theoretical models, which suggest that higher poling temperatures reduce the energy barriers for domain reorientation, thereby facilitating better alignment and polarization of the domains.

When analyzing the shape and size of the grains, it can be noticed that in the case of the base and Mn-doped samples, the grains are smaller than in the Ca and Sr-doped samples. The largest grains were observed for the Sr-doped sample. In this case, Sr doping promotes grain growth. There are fewer grain boundaries, which facilitates sample polarization (highest $_{33}$).

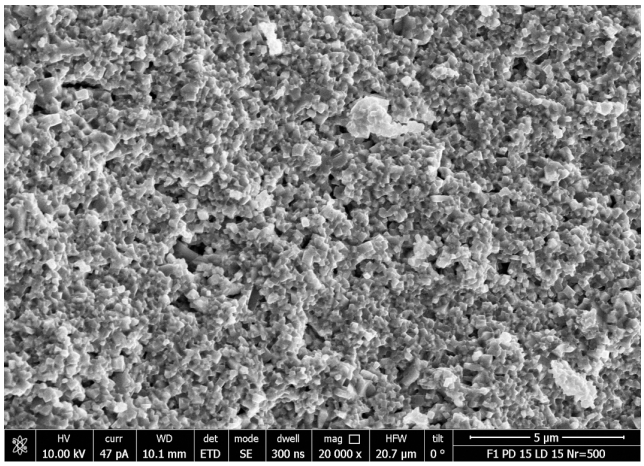

(a)

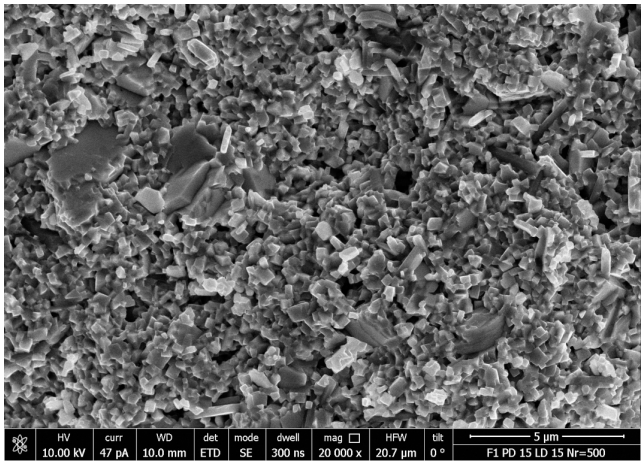

(b)

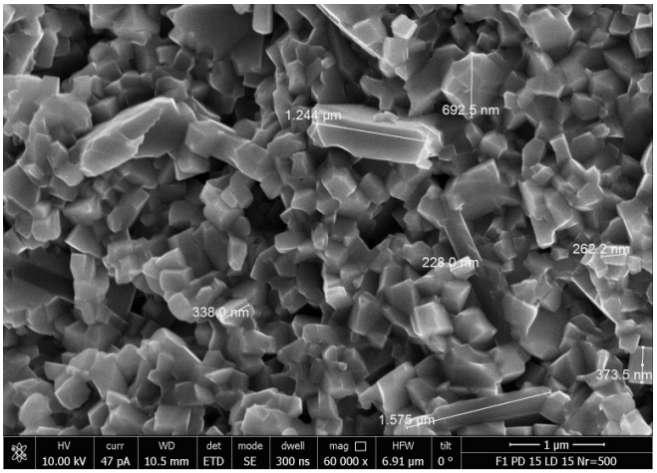

(c)

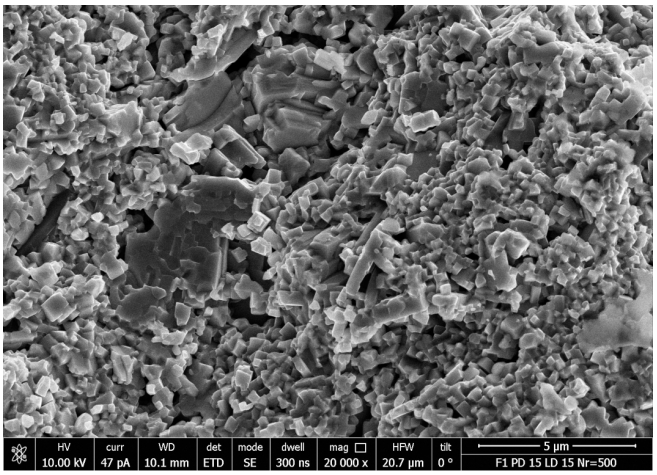

(d)

Fig. 3. SEM microstructure images for the tested materials: (a) base KBT, mag. 20k×; (b) KBT:Ca, mag. 20k×; (c) KBT:Mn, mag. 60k×; (d) KBT:Sr, mag. 20k×

In this case, domain mobility is the highest among the tested samples. Ca and Mn doping inhibits grain growth. In this case, there is a larger number of grain boundaries, which renders polarization of the structure more difficult due to the local increase in stresses in the crystal lattice. It is worth noting that the grains exhibit the highest homogeneity as compared to the other tested materials. Domain mobility for these samples is limited. During measurements of the d_{33} coefficient, it was observed that its value shows significant variation depending on the location of the measuring point, i.e. the distance from the center of the sample.

The tests were carried out on ceramic discs with a diameter of 15 mm and a thickness of 2 mm by moving the piezometer electrodes along the selected diameters, starting from the edge. The sample was placed in a specially prepared location, using 3D printing technology (FDM – Zortrax M200).

As a result, an approximate map of spatial distribution of the d_{33} coefficient on the sample surface was obtained. Example results are shown in Fig. 4a and 4b. Measurements were made along four diameters spaced 45° apart. The missing measurement points were reconstructed by the software approximation method.

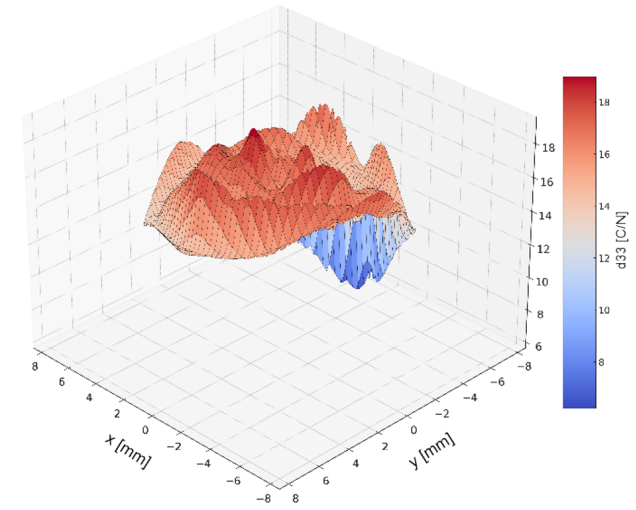

(a)

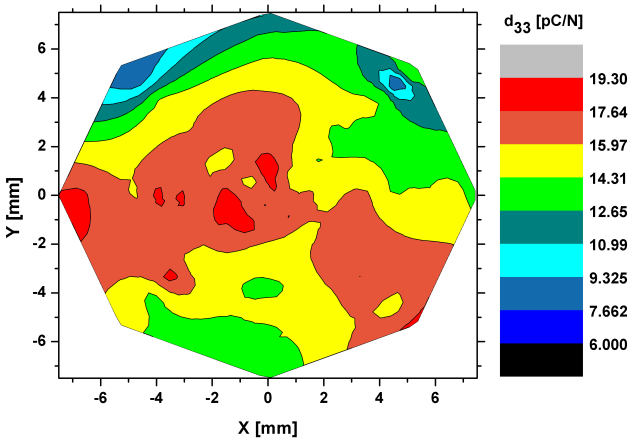

(b)

Fig. 4. (a) Example of d_{33} value distribution – 3D; (b) 2D

The obtained d_{33} distribution for the KBT base sample polarized at ambient temperature shows inhomogeneity, with values ranging from about 6 to 19 pC/N. In particular, on one part of the edge, results could be observed that were significantly different from the others. This may have been related to the process of forming the sample into a disc. Despite the use of a uniform electric field during the polarization process, differences were observed that may result from local microstructural inhomogeneities of the material. As a sintered ceramic, the tested sample is characterized by heterogeneous polycrystalline structure (Fig. 3), which may affect the piezoelectric properties.

4. CONCLUSIONS

Based on the measurements carried out, it can be concluded that each of the three applied variants of modification of the tested materials: production method, addition of dopants and increase

of temperature during the polarization process, had a significant influence on the level of the piezoelectric coefficient d_{33} value. Temperature values were selected so as not to exceed the Curie point. Studies indicate that thermal processes, such as different sintering temperatures and additives (e.g. strontium, calcium, manganese), have a significant influence on the piezoelectric properties of KBT (Tables 1–3). The microstructure of polycrystalline materials such as KBT plays a key role here. Control of the microstructure, including grain size and porosity, through thermomechanical processes opens up possibilities in shaping the functional properties of these materials. Studies have confirmed that the temperature for polarization in an electric field has a significant effect on the d_{33} values, which emphasizes the need for precise control of thermal parameters in the polarization process of piezoelectric materials. The measurements performed showed that the distribution of the d_{33} coefficient in the tested ceramic samples is non-uniform. Despite the application of a uniform electric field during the polarization process, the d_{33} value varies spatially within a single sample, suggesting the presence of local microstructural inhomogeneities. Such variability may result from the polycrystalline structure typical for ceramic materials, including, among others, non-uniform porosity distribution, grain orientation or local structural defects visible in SEM images (Fig. 3). The findings of this study may be significant for the development of high-performance, lead-free piezoelectric materials. The optimization of doping and poling conditions offers significant potential for advancing the application of KBT ceramics in piezoelectric sensors, actuators and energy harvesting devices, particularly in environmentally friendly technologies.

ACKNOWLEDGEMENTS

The studies were funded by the National Science Centre (grant No. 2018/02/X/ST5/03189 and 2021/05/X/ST5/01277). These results are part of a project funded by the European Union Horizon 2020 research and innovation program under the Marie Skłodowska-Curie Grant Agreement No. 778156. Support from the resources for science in 2018–2023, allocated for the international co-financed grant No. W13/H2020/2018 (Dec. MNiSW 3871/H2020/2018/2), is also acknowledged.

REFERENCES

[1] A. Testino, "Ceramics for electronics and energy: Issues and opportunities," *Int. J. Appl. Ceram. Technol.*, vol. 10, pp. 723–730, 2013, doi: 10.1111/ijac.12123.

[2] F. Tian, Y. Liu, R. Ma, F. Li, Z. Xu, and Y. Yang, "Properties of PMN–PT single crystal piezoelectric material and its application in underwater acoustic transducers," *Appl. Acoust.*, vol. 175, p. 107827, 2021, doi: 10.1016/j.apacoust.2020.107827.

[3] F. Zhang *et al.*, "Preparation and electrical properties of a new-type intergrowth bismuth layer-structured ceramics," *J. Alloys Compd.*, vol. 753, pp. 54–59, 2018, doi: 10.1016/j.jallcom.2018.04.134.

[4] G.W. Bailey *et al.*, "Polarization screening and image formation in SSPM, EFM and piezoresponse imaging of ferroelectric $BaTiO_3$ surfaces," *Microsc. Microanal.*, vol. 6, suppl. 2, pp. 706–707, 2000, doi: 10.1017/S1431927600036023.

[5] G.H. Heartling, "Ferroelectric ceramics: History and Technology", *J. Am. Ceram. Soc.*, vol. 2011, no. 82, pp. 797–818, 2011, doi: 10.1111/j.1151-2916.1999.tb01840.x.

[6] M. Algueró, C. Alemany, B. Jiménez, J. Holc, M. Kosec, and L. Pardo, "Piezoelectric PMN–PT ceramics from mechanochemically activated precursors," *J. Eur. Ceram. Soc.*, vol. 24, no. 6, pp. 1593–1598, 2004, doi: 10.1016/S0955-2219(03)00598-3.

[7] Y. Wu *et al.*, "Influence of tungsten doping on dielectric properties of strontium bismuth niobate ceramics," *J. Mater. Sci. Lett.*, vol. 21, no. 12, pp. 947–949, 2002, doi: 10.1023/A:1016077724427.

[8] H. Chen *et al.*, "Donor and acceptor doping effects on the electrical conductivity of $CaBi_2Nb_2O_9$ ceramics," *Phys. Status Solidi A*, vol. 210, no. 6, pp. 1121–1127, 2013, doi: 10.1002/pssa.201228804.

[9] T. Haccart, E. Cattan, and D. Remiens, "Dielectric, ferroelectric and piezoelectric properties of sputtered PZT thin films," *Semicond. Phys. Quantum Electron. Optoelectron.*, vol. 5, no. 1, pp. 78–88, 2002.

[10] V.V. Deshmukh *et al.*, "Structure, morphology and electrochemical properties of SrTiO[2083?] perovskite," *Environ. Chem. Ecotoxicol.*, vol. 3, pp. 241–248, 2021, doi: 10.1016/j.enece.2021.03.002.

[11] S.H. Baek, M.S. Rzchowski, and V.A. Aksyuk, "Giant piezoelectricity in PMN–PT thin films: Beyond PZT," *MRS Bull.*, vol. 37, pp. 1022–1029, 2012, doi: 10.1557/mrs.2012.266.

[12] L. Liu *et al.*, "Piezoelectric properties of BiFeO[2083?] exposed to high temperatures," *Adv. Funct. Mater.*, vol. 34, no. 21, 2024, doi: 10.1002/adfm.202314807.

[13] D. Czekaj, A. Lisińska-Czekaj, D. Foryś, and Z. Surowiak, "Application of thermal analysis to determine technological conditions for ferroelectric ceramics fabrication," *Ceramics*, vol. 80, pp. 451–456, 2003.

[14] S.K. Pandey, "Structural, ferroelectric and optical properties of PZT thin films," *Physica B*, vol. 369, pp. 135–142, 2005, doi: 10.1016/j.physb.2005.08.024.

[15] M. Acosta *et al.*, "BaTiO[2083?]-based piezoelectrics: Fundamentals, current status, and perspectives," *Appl. Phys. Rev.*, vol. 4, p. 041305, 2017, doi: 10.1063/1.4990046.

[16] D.Q. Xiao, D. Lin, J. Zhu, and P. Yu, "Studies on new systems of BNT-based lead-free piezoelectric ceramics," *J. Electroceram.*, vol. 21, pp. 34–38, 2008, doi: 10.1007/s10832-007-9087-5.

[17] H. Nagata *et al.*, "Piezoelectric properties of bismuth sodium titanate ceramics," *Ceram. Trans.*, vol. 167, pp. 213–221, 2005, doi: 10.1002/9781118408186.ch20.

[18] D.-J. Shin, J. Kim, S.-J. Jeong, and J.-H. Koh, "Piezoelectric and ferroelectric properties in $Ba(Zr,Ti)O_3$ ceramics," *Mater. Res. Bull.*, vol. 82, pp. 123–130, 2016, doi: 10.1016/j.materresbull.2016.03.003.

[19] S. Mishra and P. Kumar, "Enhanced dielectric and piezoelectric properties of BZT–BCT system near MPB," *Ceram. Int.*, vol. 40, no. 9, pp. 14057–14063, 2014, doi: 10.1016/j.ceramint.2014.06.001.

[20] P. Czaja *et al.*, "Lead-free ceramics based on potassium–bismuth titanate $K_{0.5}Bi_{0.5}TiO_3$," *2D and Quasi-2D Composite and Nanocomposite Materials*, pp. 149–161, 2020, doi: 10.1016/B978-0-12-818819-4.00013-1.

[21] J. Suchanicz *et al.*, "Structural, thermal, dielectric and ferroelectric properties of $K_{0.5}Bi_{0.5}TiO_3$ ceramics," *J. Eur. Ceram. Soc.*, vol. 38, no. 2, pp. 567–574, 2018, doi: 10.1016/j.jeur ceramsoc.2017.09.036.

[22] R. Maalal, D. Mercurio, G. Trolliard, and J.-P. Mercurio, "Crystal structure and dielectric properties of mixed Aurivillius phases," *Ann. Chim. Sci. Mat.*, vol. 23, p. 247–250, 1998, doi: 10.1016/S0151-9107(98)80066-4.

[23] A. Tuluk, Tadhg Mahon, Sybrand van der Zwaag, Pim Groen, "Estimating the true piezoelectric properties of $BiFeO_3$ from measurements on $BiFeO_3$-PVDF terpolymer Composites," *J. Alloys Compd.*, vol. 868, p. 159186, 2021, doi: 10.1016/j.jallcom.2021.159186.

[24] G. Picht, V. Bouvier, S. Frank, J. Koruza, F. Felten, and G. Lindemann, "Ferroelastic Properties of PZT: Characterization under Compressive and Tensile Stress, Finite-Element Simulation, and Lifetime Calculation," *IEEE Trans. Ultrason. Ferroelectr. Freq. Control*, vol. 65, no. 9, pp. 1542–1551, Sept. 2018, doi: 10.1109/TUFFC.2018.2860784.

[25] K. Liu *et al.*, "Effect of the slurry composition on the piezoelectric properties of PZT ceramics fabricated via materials extrusion 3D printing," *Ceram. Int.*, vol. 49, no. 12, pp. 20024–20033, 2023, doi: 10.1016/j.ceramint.2023.03.124.

[26] J. Zhang, P. Pan, P. Jiang, J. Qin, and J. Hu, "Electric degradation in PZT piezoelectric ceramics under a DC bias," *Sci. Eng. Compos. Mater*, 27, pp. 464–468, 2020, doi: 10.1515/secm-2020-0049.

[27] T.R. Shrout and S.J. Zhang, "Lead-free piezoelectric ceramics: Alternatives for PZT," *J. Electroceram.*, vol. 19, pp. 111–124, 2007.

[28] M.I. Haque Ansari, A. Qurashi, and M.K. Nazeeruddin, "Frontiers, opportunities and challenges in perovskite solar cells: A critical Reviews," *J. Photochem. Photobiol. C*, vol. 35, pp. 1–24, 2018, doi: 10.1016/j.jphotochemrev.2017.11.002.

[29] D. Bochenek, J. Dudek, and Z. Surowiak, "Influence of the poling conditions on the stability of work o feroceramics transducers based on the PZT," *Ceramics*, vol. 80, pp. 439–444, 2003.

[30] P. Czaja, J. Suchanicz, D. Bochenek, W. Piekarczyk, P. Jeleń, and J. Michniowski, "Influence of milling time on the synthesis, microstructure and mechanical properties of lead-free $K_{0.5}Bi_{0.5}TiO_3$ ceramics," *Integr. Ferroelectr.*, vol. 196, no. 1, pp. 105–111, 2019, doi: 10.1080/10584587.2019.1591969.

[31] P. Czaja, J. Suchanicz, D. Bochenek, G. Dercz, M. Piasecki, and W. Hudy, "High density lead-free $K_{0.5}Bi_{0.5}TiO_3$ ceramics: preparation, mechanical and dielectric properties," *Phase Trans.*, vol. 9, no. 9–10, pp. 1051–1059, 2018, doi: 10.1080/0141 1594.2018.1509974.

[32] M. Otoničar, S.D. Škapin, B. Jančar, R. Ubic, and D. Suvorov, "Analysis of the phase transition and the domain structure in K0.5Bi0.5TiO3 perovskite ceramics by in situ XRD and TEM," *J. Am. Ceram. Soc.*, vol. 93, no. 12, pp. 4168–4173, 2010, doi: 10.1111/j.1551-2916.2010.04013.x.